

Architectural design of the pelvic floor is consistent with muscle functional subspecialization

Lori J. Tuttle · Olivia T. Nguyen · Mark S. Cook ·
Marianna Alperin · Sameer B. Shah · Samuel R. Ward ·
Richard L. Lieber

Received: 24 April 2013 / Accepted: 6 July 2013
© The International Urogynecological Association 2013

Abstract

Introduction and hypothesis Skeletal muscle architecture is the strongest predictor of a muscle's functional capacity. The purpose of this study was to define the architectural properties of the deep muscles of the female pelvic floor (PFMs) to elucidate their structure–function relationships.

Methods PFMs coccygeus (C), iliococcygeus (IC), and pubovisceral (PV) were harvested en bloc from ten fixed

human cadavers (mean age 85 years, range 55–102). Fundamental architectural parameters of skeletal muscles [physiological cross-sectional area (PCSA), normalized fiber length, and sarcomere length (L_s)] were determined using validated methods. PCSA predicts muscle-force production, and normalized fiber length is related to muscle excursion. These parameters were compared using repeated measures analysis of variance (ANOVA) with post hoc *t* tests, as appropriate. Significance was set to $\alpha=0.05$.

Results PFMs were thinner than expected based on data reported from imaging studies and in vivo palpation. Significant differences in fiber length were observed across PFMs: C=5.29±0.32 cm, IC=7.55±0.46 cm, PV=10.45±0.67 cm ($p<0.001$). Average L_s of all PFMs was short relative to the optimal L_s of 2.7 μm of other human skeletal muscles: C=2.05±0.02 μm , IC=2.02±0.02 μm , PC/PR=2.07±0.01 μm ($p=<0.001$ compared with 2.7 μm ; $p=0.15$ between PFMs, power=0.46). Average PCSA was very small compared with other human muscles, with no significant difference between individual PFMs: C=0.71±0.06 cm^2 , IC=0.63±0.04 cm^2 , PV=0.59±0.05 cm^2 ($p=0.21$, power=0.27). Overall, C had shortest fibers, making it a good stabilizer. PV demonstrated the longest fibers, suggesting that it functions to produce large excursions.

Conclusions PFM design shows individual muscles demonstrating differential architecture, corresponding to specialized function in the pelvic floor.

Keywords Muscle architecture · Muscle function · Pelvic floor

L. J. Tuttle
Department of Orthopaedic Surgery, University of California San Diego, San Diego, CA, USA

O. T. Nguyen
Department of Bioengineering, University of California San Diego, San Diego, CA, USA

M. S. Cook
Department of Integrative Biology and Physiology, University of Minnesota, Minneapolis, MN, USA

M. Alperin
Department of Reproductive Medicine, Division of Female Pelvic Medicine and Reconstructive Surgery, University of California San Diego, San Diego, CA, USA

S. B. Shah
Departments of Orthopaedic Surgery and Bioengineering, University of California San Diego, San Diego, CA, USA

S. R. Ward
Departments of Radiology, Orthopaedic Surgery and Bioengineering, University of California San Diego, San Diego, CA, USA

R. L. Lieber (✉)
Departments of Orthopaedic Surgery and Bioengineering, University of California San Diego, 9500 Gilman Drive, Mail Code 0863, La Jolla, CA 92093, USA
e-mail: rlieber@ucsd.edu

R. L. Lieber
VA San Diego Healthcare System, San Diego, CA, USA

Introduction

Immediate trauma to the pelvic floor is a serious and common complication of vaginal childbirth and is the greatest risk factor for development of pelvic floor dysfunction [1].

The cost of pelvic floor disorders (PFD) exceeds 1 billion dollars per year, with >300,000 patients annually in the United States requiring corrective surgery [2]. Trauma to the pelvic floor muscles (PFMs) appears to play an important role in the pathogenesis of PFD. Defects in the levator ani complex have been demonstrated in one third of women after spontaneous vaginal delivery and in 60 % after forceps-assisted delivery [3]. The risk of developing PFD is dramatically increased when injury to PFMs or nerves is visibly present on imaging studies [4]. Despite this association, baseline architectural parameters—which determine functional capacity—of PFMs remain unknown.

Skeletal muscle architecture, defined as the arrangement of muscle fibers relative to the axis of force generation, is the primary predictor of muscle function [5]. It governs the magnitude of force a muscle can generate, how fast it contracts (velocity), and its active range (excursion). Other parameters, such as fiber-type distribution, can modulate contractile properties, but they are relative values and cannot be converted to muscle-force values (in N) or muscle excursions (in m). Thus, definition of a muscle's architecture can add to the understanding of its mechanical function and susceptibility to muscle injury. Measures of muscle architecture include fiber length (L_f), the determinant of excursion; physiological cross-sectional area (PCSA), the predictor of force generation; and sarcomere length, which determines the relative isometric force a muscle generates when activated at a particular length [6]. Muscles with large PCSA and short fibers are optimized for stabilization; muscles with small PCSA and long fibers are optimized for maximum excursion [7]. In orthopedics, muscle architecture can be used to choose therapeutic interventions that best improve muscle function postinjury [8]. For example, muscle architecture has been used to determine the most appropriate muscle to use in a tendon transfer to improve hand and arm function in people living with spinal cord injury [8]. Despite the high prevalence of PFM injury and its level of morbidity, it is surprising that PFM architectural characterization is not

available beyond a study of a single cadaveric specimen [9]. Understanding PFM architecture is the necessary first step to allow determination of the structural basis of PFM function and provide insights into PFD. Ultimately, this information can be used to develop effective rehabilitation strategies for PFM injuries secondary to vaginal delivery. Thus, the purpose of this study was to define and compare the architecture of the individual components of the deep pelvic floor striated muscles—coccygeus, iliococcygeus, and pubovisceral—in cadaveric human specimens and thus understand their functional capacity.

Materials and methods

Cadaveric specimens were obtained courtesy of the University of Minnesota Bequest Program, and this work was exempt from institutional review board approval due to exclusion of living subjects. Select demographic data and bony pelvis measurements are summarized in Table 1.

Pelvic floor muscle dissection

Muscles of the pelvic floor were removed en bloc from ten fixed human female cadavers with no known history of pelvic floor injury or dysfunction. The fixative solution consisted of 70 % isopropyl alcohol, 13 % phenol, 8 % formaldehyde, 8 % sorbitol, and 1 % BARQUAT MB-50 disinfectant. The solution was diluted to 50 % with water. The bodies were perfused with the solution by accessing the common carotid and common femoral arteries in a supine position. Depending on size, 8–14 gallons of solution were delivered. The gluteus maximus muscle was reflected and the sacrotuberous ligament identified. Fat and connective tissue were removed from the ischiorectal fossa, and pelvic organs were removed to reveal the tendinous attachments of levator ani muscles. The tendinous arc of the levator ani was gently detached from the obturator fascia. The sacrotuberous ligament was removed

Table 1 Demographic and anatomic characteristics

Donor	Age (years)	BMI (kg/m ²)	Parity	Bony pelvic dimensions (transverse x coronal cm)
1	100	12.2	2	12.1 × 12.1
2	87	18.5	1	11.9 × 11.4
3	69	17.3	NA	15.3 × 13.5
4	99	16.0	NA	13.8 × 12.8
5	89	19.5	NA	13.2 × 13.7
6	55	18.1	2	14.2 × 14.1
7	96	17.7	NA	13.5 × 13.0
8	102	18.6	NA	13.3 × 10.1
9	95	18.3	NA	13.8 × 13.5
10	60	20.0	5	13.8 × 12.1

BMI body mass index, NA not available

and the pudendal neurovascular bundle reflected to expose the sacrospinous ligament. The sacrum was cut at the inferior edge of the piriformis, and the sacrospinous ligament was cut at the attachment to the ischial spine, effectively detaching the pelvic diaphragm posteriorly and laterally. The anterior attachment of the levator ani from the pubic bone was detached, and the pelvic diaphragm was then removed en bloc from the pelvis. The pelvic inlet was measured in the transverse and coronal plane [9]. To facilitate dissection, specimens were cut anteriorly from the pubic symphysis down the midline, through the urogenital hiatus, and inferiorly into the anal opening, which resulted in a trapezoidal specimen containing the PFMs (Fig. 1a). To improve visualization of individual PFMs, we obtained high-resolution photographs of each specimen from superior and inferior view (Figs. 1a, b). We isolated the coccygeus, iliococcygeus, and pubovisceral muscles (Fig. 1c) from each other by following fibers from the origin and insertion points, as outlined by Kearney et al. [10]. All final divisions were made in consultation with a urogynecologist and after two senior investigators agreed on the boundaries. To permit subjective demonstration of muscle thickness, we obtained high-resolution photos of each specimen under conditions of rear illumination (Fig. 1d).

Muscle architecture measures

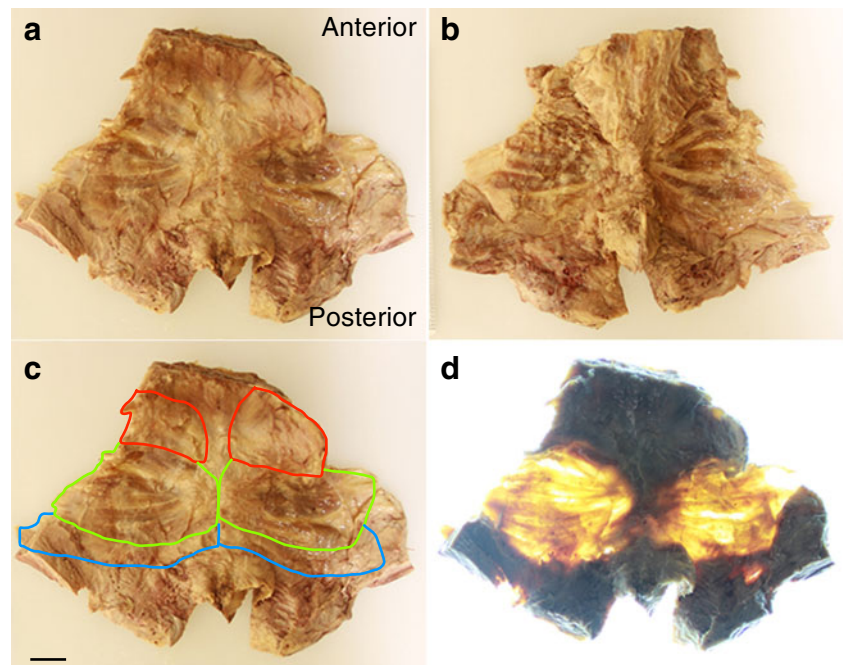
Muscle architecture was characterized according to the method originally developed by Sacks and Roy [11] and previously applied to human muscle by Lieber et al. [12]. Connective tissue and fat were removed from each muscle

before it was weighed. Each muscle was divided into three regions (cephalad, middle, caudate), and three random fascicles (bundles of ~100 fibers) were dissected from each region for architectural measurements. Fascicles were measured using electronic digital calipers to the nearest 0.01 mm. If fascicles were not oriented in a way that could accurately be measured with a caliper (such as curved fibers), a suture was used to follow the fiber length, and suture length was then measured. Each fascicle was immersed in a 15 % sulfuric acid solution for at least 30 min to partially digest intramuscular connective tissue. Under a binocular dissecting microscope and with the use of surgical forceps, smaller fiber bundles (approximately 10–20 fibers) were teased from the fascicle and placed on a glass slide to measure sarcomere length. Sarcomere length was measured by laser diffraction according to the method described by Lieber et al. [13]. Data from a fiber was only used if at least three useable sarcomere lengths were obtained. All architecture measurements were performed by the same two investigators.

Positional differences at the time of death and fixation can alter fiber length. To circumvent this complication, we normalized fiber length using the method validated by Felder et al. [14]. Fiber lengths were normalized using the equation $L_f = L_f' (2.7 \mu\text{m}/L_s)$ where L_f' is the raw fiber length, L_s is the measured sarcomere length, L_f is normalized fiber length, and $2.7 \mu\text{m}$ represents optimal sarcomere length in human muscle [12]. Finally, PCSA, the best predictor of muscle force, was calculated using the following formula:

$$PCSA = \frac{m \cdot \cos\theta}{\rho \cdot L_f}$$

Fig. 1 Pelvic floor muscles dissected en bloc (**a,b**) from superior and inferior views, respectively, with superimposed boundaries of coccygeus (C; red), iliococcygeus (IC; green), and pubovisceral (PV; blue) (**c**), and rear illuminated (**d**). Scale bar=2 cm for all images



where m is mass, θ is the pennation angle (negligible in these muscles, as pennation angle is measured relative to a muscle's internal tendon and the PFM do not have internal tendons), ρ is muscle density (1.056 g/cm^3 [15]), and L_f is normalized muscle-fiber length. To predict maximum isometric-force production, PCSA was multiplied by mammalian skeletal muscle specific tension for fast (23.5 N/cm^2) and slow (17.2 N/cm^2) fibers [16] weighted for the average fiber type percentage of human muscles (35 % fast, 65 % slow) [17].

Apparent thickness estimate

Using the pelvic dimensions measured in each cadaver (Table 1) and the volume of PFMs, an apparent thickness of each specimen was calculated. PFMs were assumed to occupy an anatomic area of 70 % of pelvic inlet measurements. PFM volume was calculated by dividing total muscle mass per specimen by the density of fixed tissue (1.056 g/cm^3). Dividing muscle volume by anatomical area provided an apparent thickness measure.

Collagen content

Muscle mass is a primary component of the PCSA calculation and, to accurately calculate PCSA, should reflect only muscle contractile components. Contributions of muscle connective tissue could artificially inflate PCSA values. To account for the intramuscular extracellular matrix, we measured collagen content, a major constituent of the extracellular matrix, and scaled our PCSA values appropriately. Hydroxyproline content was used to determine collagen percentage using a modification of a previously validated protocol [18]. Small tissue samples (2 mg) were taken from nine regions of each muscle and hydrolyzed in 6 N hydrochloric acid (HCl) at 110°C for 24 hs. Samples were then pipetted with standards into 96-well plates and incubated with a chloramine T solution for 20 min at room temperature, followed by the addition of a p-dimethylaminobenzaldehyde solution and incubated at 60°C for 30 min. Hydroxyproline concentration was determined by spectrophotometry at 550 nm and normalized to the mass of the original tissue sample.

Statistical analysis

Repeated measures analysis of variance (ANOVA) was used to compare mean PCSA, fiber length, and sarcomere length among the different muscles, with post hoc t tests, as appropriate. Significance was set to $\alpha=0.05$. Results are presented as means \pm standard error of the mean (SEM), except where noted. All statistical analyses were performed using GraphPad Prism version 5.00, GraphPad Software, San Diego, CA, USA.

Results

The PFM was subjectively much thinner than anticipated—essentially the PFM consisted of thin muscle fascicles encased in sheets of connective tissue, with fat and connective tissue interspersed between and within the muscles (Fig. 1). Based on our clinical experience, in vivo vaginal palpation of the presumed levator ani muscles, and the appearance of these muscles in published images, we expected PFMs to have significantly more bulk than what was found. We placed the specimens on a light box for photographs and confirmed that portions of PFMs are thin to the point where light easily passes through the muscles (Fig. 1). Average apparent thickness, of our specimens was calculated to be $2.4 \text{ mm} \pm 0.6$. There were no systematic differences between right and left sides, and there were no regional differences in the cephalad, middle, and caudate regions of the individual muscles. Thus, our presentation of results refers to each aggregate muscle.

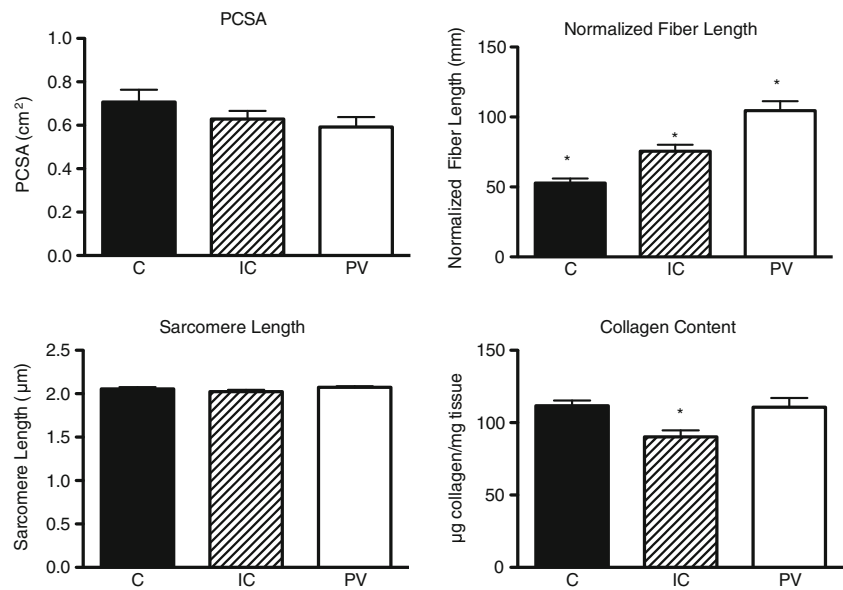
Significant differences were observed across individual components of PFMs for fiber length, but there was no significant PCSA or sarcomere length difference among muscles (Fig. 2). Average PCSA without adjusting for collagen content was coccygeus (C) = $0.71 \pm 0.06 \text{ cm}^2$, iliococcygeus (IC) = $0.63 \pm 0.04 \text{ cm}^2$, pubovisceral (PV) = $0.59 \pm 0.05 \text{ cm}^2$ $P=0.21$, power = 0.27). These PCSA values are small compared with other skeletal muscles [19], indicating they would produce relatively small forces. All three muscles were significantly different from one another in normalized fiber length (C = $5.29 \pm 0.32 \text{ cm}$, IC = $7.55 \pm 0.46 \text{ cm}$, PV = $10.45 \pm 0.67 \text{ cm}$ $P < 0.001$), indicating the PV muscle is capable of producing the largest excursion. Average sarcomere length was not significantly different among muscles and was very short (C = $2.05 \pm 0.02 \text{ }\mu\text{m}$, IC = $2.02 \pm 0.02 \text{ }\mu\text{m}$, PV = $2.07 \pm 0.01 \text{ }\mu\text{m}$ $P=0.15$, power = 0.46) compared with the optimal human sarcomere length of $2.7 \text{ }\mu\text{m}$ and to other reported sarcomere lengths for human extremity muscles [12, 19].

Collagen content was similar between C and PV muscles, and both had greater collagen content than the IC muscle (C = $111.7 \pm 3.6 \text{ }\mu\text{g/mg}$, IC = $90.23 \pm 4.5 \text{ }\mu\text{g/mg}$, PV = $110.7 \pm 6.4 \text{ }\mu\text{g/mg}$ $P=0.01$) (Fig. 2). Thus, PFMs contain 9–11 % collagen, which is significantly higher than the <3 % found in other human skeletal muscles [17]. PCSA corrected for collagen content yields mean values of C = 0.63 cm^2 , IC = 0.67 cm^2 , PV = 0.53 cm^2 . Based on these values and the presumed fiber type percentage of PFMs of 65 % type 1 and 35 % type 2 fibers [17], these muscles would be predicted to produce about 10.3–12.9 N of force individually and 35.4 N combined.

Discussion

Here we report the fundamental architectural parameters of skeletal muscles of the female pelvic floor, which allows us

Fig. 2 Structural and biochemical properties of human pelvic floor muscles. Values are means \pm standard error of the mean (SEM). * Muscle that is different from the other two muscles ($P=0.05$). *PCSA* physiological cross-sectional area, *C* coccygeus muscle, *IC* iliococcygeus muscle, *PV* pubovisceralis muscle



to define their functional properties. In the field of orthopedic surgery, significant advances in treating muscular dysfunction have occurred since muscle architecture, physiology, and pathophysiology were established [8]. This study represents the first step in a series of these types of experiments aimed at elucidating the above characteristics for PFMs.

Complexity of PFM function lies in their two main purposes: to provide support to the viscera, constricting urethra, vagina, and anal canal, and at the same time allowing movement of contents from one cavity to another (urination, defecation, parturition). We found that PFM architectural design is unique for their dual function. Specifically, PFMs have smaller PCSAs compared with other skeletal muscles around the pelvis. For example, the multifidus muscle, which is designed as a stabilizer of the spine, has a mean PCSA of 23.9 cm² [20], which is >30 times the PCSA of PFMs. Muscles of the abdominal wall, such as the rectus abdominis and transverse abdominis, which generate intra-abdominal pressure in conjunction with the diaphragm, have PCSAs of 2.8 and 5.2 cm², respectively, [21], which is four to seven times the PCSA of PFMs. Based on our clinical experience, in vivo vaginal palpation of the presumed levator ani muscles, and the appearance of these muscles in published images, we expected PFMs to have significantly more bulk than what was found (2.41 mm \pm 0.6). Imaging techniques and clinical examinations have limited resolution by which to visualize thin structures, such as PFMs, and particularly by which to distinguish between contractile and connective tissue components of individual muscles, which may account for the differences in our results.

Architectural parameters predict that muscles with long fiber lengths produce large excursions (elongation and contraction). We found the longest fibers in the pubovisceral component of

the levator ani complex, which is a perfect design for a muscle that needs to facilitate activities such as defecation and pelvic floor distention in response to increased abdominal pressure. Compared with other skeletal muscles, the PV has a mean fiber length of 10.5 cm, whereas the transverse abdominis portion of the abdominal wall, for example, has a mean fiber length of 9.5 cm [21]. As expected, the largest PCSA and shorter fiber lengths were found in C, making it a good stabilizer of the coccyx, which can impact pelvic floor function (Fig. 3). Although sarcomere lengths were not significantly different among individual muscles, they were all short compared with the optimal sarcomere length of 2.7 μ m for human skeletal muscles [12]. This suggests that PFMs can produce more force when stretched because sarcomere length is increasing toward the plateau of the length–tension curve, which would be mechanically advantageous to these muscles that must counteract increases in intra-abdominal pressure and continuously resist elongation during normal use [22].

One of the most practical applications of quantitative architectural data is to predict muscle function under various conditions. The tension generated by PFMs, based on their geometry, is related to their radius of curvature (based on the interspinous distance of the pelvis) by the Law of Laplace for a spherical vessel [23]. In terms of muscle stress (σ), intra-abdominal pressure (P), and PFM thickness (t), this relationship is given as:

$$\sigma = \frac{Pr}{2t}$$

which, to balance equations of motion, must also be equal to the tension generated by the muscle (T) divided by the cross-sectional area of PFMs generating the tension, assuming that only PFMs are resisting intra-abdominal pressure in this

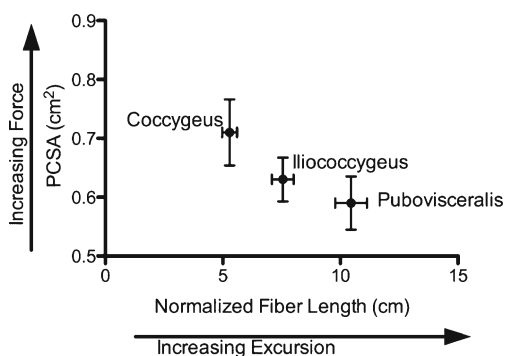


Fig. 3 Normalized fiber length and physiological cross-sectional area [physiological cross-sectional area (PCSA)] for human pelvic floor muscles (PFMs). Values are means ± standard error of the mean (SEM)

system. Thus, another expression for muscle stress is given by:

$$\sigma = \frac{T}{2\pi r t}$$

Equating these two expressions and solving for intra-abdominal pressure yields:

$$P = \frac{T}{\pi r^2}$$

Using this relationship, it is possible to relate experimentally measured intra-abdominal pressure to the predicted

Table 2 Reported mean values for intra-abdominal pressure based on activity

Activity	Intra-abdominal pressure (kPa)	Reference
Basal	0.24-0.85	[24]
Basal term pregnancy	2.9	[25]
Sitting	2.2	[24]
Standing	2.7	[24]
Abdominal crunch	3.6	[24]
Valsalva	5.3	[24]
Weighted squat (15 kg)	7.8	[26]
Cough	4.9–10.8	[24, 27]
Jumping	22.8	[24]

tension generated by PFMs. *P* values from the literature during normal activities range more than 100-fold, from 0.24–23 kPa (Table 2). As described above, we predict that the maximum isometric tension for these muscles is ~35 N and, based on pelvic floor dimensions, the radius of musculature curvature is ~5 cm (0.05 m) [28]. Of course, each of these parameters is associated with some uncertainty, so we performed a sensitivity analysis over the possible radius values of 4–6 cm and tetanic tension values of 20–40 N to calculate the intra-abdominal pressure that can be resisted by the muscles. This range of values accounts for pelvic size variation and potential effects

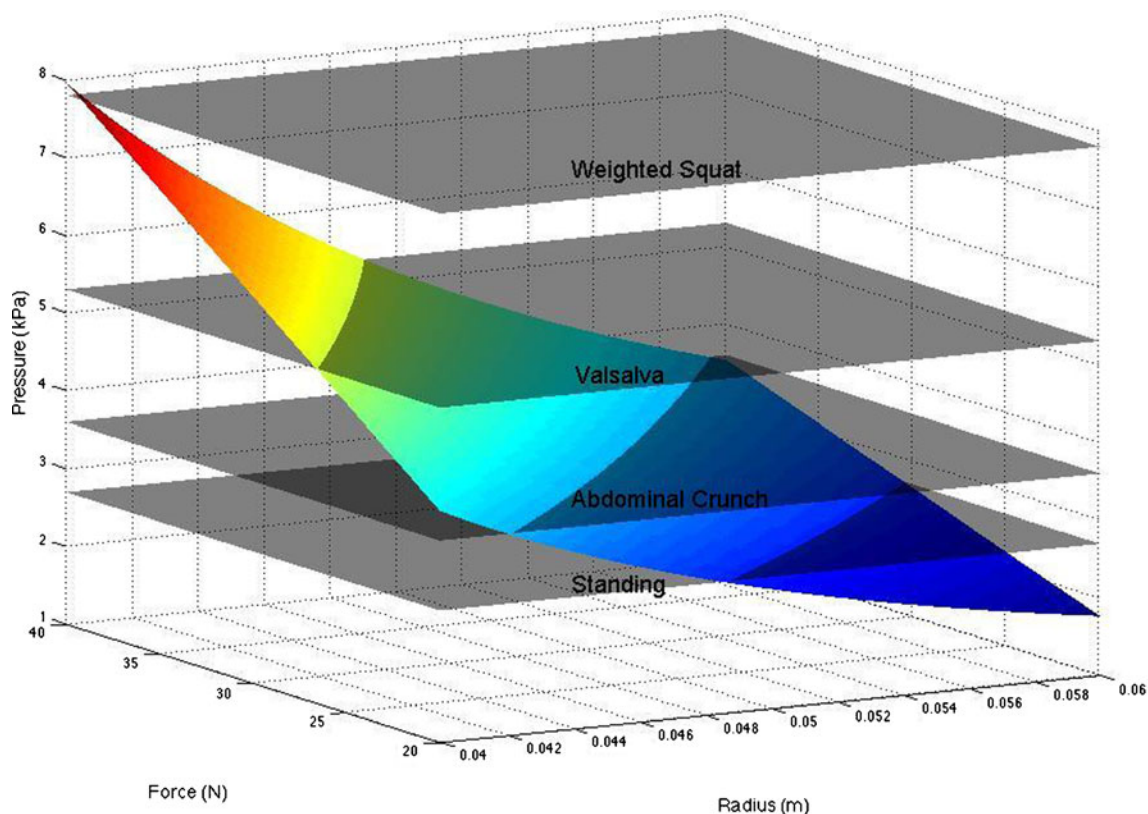


Fig. 4 Sensitivity analysis varying pelvis dimensions, muscle tension, and pressure

of muscle atrophy that is likely to be present in these aged specimens. Sensitivity analysis data are plotted in Fig. 4, along with sample “planes” of pressure from the literature.

It can be seen that for activities of daily living, PFMs can generate sufficient tension to oppose intra-abdominal pressure. However, for more severe events (voluntary cough, jump, etc.), intra-abdominal pressure clearly exceeds the maximum tension generated by these muscles. Even if the muscles are forced to lengthen during contraction, which can enhance their force by about twofold [29], they cannot withstand these pressures. This result strongly implies that other parallel structures are required to endure these more strenuous events. Possible candidates for such support structures are connective tissue components surrounding the contractile muscle components, and fascial attachments. It is also possible that PFM contraction could allow some of the load to be born by the bony pelvic ring or through compensatory muscle actions of the obturator internus via fascial attachments. However, this is speculation and requires further investigation.

This is the first time that the fundamental architectural parameters of PFM skeletal muscles have been determined by utilizing well-established and validated methods. A previous study attempted to characterize the architectural properties of the female pelvic floor [9] but only used one cadaveric specimen. We expanded on that work by analyzing muscles from ten bodies in order to provide confidence intervals for our measurements and make our average results more generalizable. Our absolute PCSA and fiber-length values are different than those in the study of Janda et al. [9], but trends in differences between individual PMF components are similar. The main difference in our findings compared with those of Janda et al. is that we found a shorter average sarcomere length than the average sarcomere length they report. It is possible that this variation is because their data come from a single donor and ours are an average of ten specimens.

We measured PFM collagen content to quantify the amount of connective tissue and calculate PCSA, which depends on the contractile mass of the specimen. The intramuscular connective tissue component is significant in PFMs, which means that traditional PCSA measures that rely only on specimen mass will overestimate force-producing capacity of these muscles by about 15 % if the noncontractile component is not subtracted. Interestingly, we found the amount of connective tissue in PFMs to be at least three times that of other skeletal muscles [17], suggesting that PFM intramuscular extracellular matrix may be relatively more important in the function of these muscles compared with extremity muscles. An understanding of how extracellular matrix interacts with these muscles to yield passive tension is extremely important. For example, if the extracellular matrix is relatively stiff and organized to “engage” at relatively short sarcomere length (low muscle strains), then the matrix could act as a checkrein, thereby generating exponentially higher muscle forces than

could be generated by active tension alone. This would explain the relative lack of active force-generating capacity observed in our sensitivity analysis and would explain why PFM injury could be catastrophic, leading to PFD.

This study has several limitations. First, our specimens were cadaveric and fixed, and therefore, the loss of resting muscle activity and intra-abdominal pressure changes the position of the pelvic floor compared with *in vivo*. Different positions of the pelvis at the time of death and fixation could alter the architectural parameters measured in our study. To circumvent this issue, we normalized fiber length to sarcomere length, which allowed us to accurately compare muscles despite differences in position due to death and fixation [14]. Another limitation of our study is the advanced age of our specimens (mean age 85 years) and the lack of consistent data on the number and mode of deliveries. At this time, it is unclear whether data from older specimens generalize to the younger or to the nulliparous population, although there is evidence from imaging data in humans that age is not a major factor in levator ani atrophy [30]. It is possible that muscle atrophy of up to 50 % could have been present due to aging [31], which is why we performed our sensitivity analysis to account for this potential factor. It is also possible that the high proportion of connective tissue in PFMs in our study represents fibrosis in these muscles as a result of birth trauma and does not represent uninjured PFMs. It is important to ultimately perform an analogous study of specimens from a younger age group with a known parous history, although new methods would need to be developed to perform this experiment properly and with minimum disruption to tissues. We are in the process of collecting these data to make comparisons to a population that may be more consistent with those seen clinically.

Despite these limitations, this study provides the first report of the skeletal muscle architectural properties of PFMs. These data predict functional subspecialization in the individual components of the PFM and parallel differences in the design of these muscles. A shift in architectural parameters due to injury will almost certainly impact the functional capacity of these muscles. Understanding and applying data from our study may lead to improved surgical and conservative rehabilitation of these muscles.

Acknowledgments This work was supported in part by NIH Grant R24 HD 50837 and by the Department of Veterans Affairs, Veterans Health Administration, Office of Research and Development, Senior Research Career Scientist Award. A portion of this work was presented in poster format at The American Urogynecology Society annual meeting (October 2012) and at the American Physical Therapy Association’s Combined Sections Meeting (January 2013).

Conflicts of interest None.

References

1. Allen RE et al (1990) Pelvic floor damage and childbirth: a neurophysiological study. *BJOG: Int J Obstet Gynaecol* 97:770–779
2. Subak LL et al (2001) Cost of pelvic organ prolapse surgery in the United States. *Obstet Gynecol* 98(4)
3. Kearney R et al (2010) Levator ani injury in primiparous women with forceps delivery for fetal distress, forceps for second stage arrest, and spontaneous delivery. *Int J Gynaecol Obstet: Off Organ Int Fed Gynaecol Obstet* 111:19–22
4. DeLancey JO et al (2007) Comparison of levator ani muscle defects and function in women with and without pelvic organ prolapse. *Obstet Gynecol* 109(2, Part 1):295–302
5. Magnaris CN, Baltzopoulos V, Sargeant AJ (1998) In vivo measurements of the triceps surae complex architecture in man: implications for muscle function. *J Physiol* 604–614
6. Powell PL, Roy RR, Kanim PP, Bello MA, Edgerton VR (1984) Predictability of skeletal muscle tension from architectural determinations in Guinea Pig Hindlimbs. *J Appl Physiol* 57:1715–1721
7. Lieber RL, Fridén J (2000) Functional and clinical significance of skeletal muscle architecture. *Muscle Nerve* 23:1647–1666
8. Lieber RL (1993) Skeletal muscle architecture: implications for muscle function and surgical tendon transfer. *J Hand Ther: Off J Am Soc Hand Ther* 6:105–113
9. Janda S, Van Der Helm F, De Blok SB (2003) Measuring morphological parameters of the pelvic floor for finite element modelling purposes. *J Biomech* 749–57
10. Kearney R, Sawhney R, DeLancey JOL (2004) Levator ani muscle anatomy evaluated by origin-insertion Pairs. *Obstet Gynecol* 104(1):168–173
11. Sacks RD, Roy RR (1982) Architecture of the hind limb muscles of cats: functional significance. *J Morphol* 173:185–195
12. Lieber RL, Fazeli BM, Botte MJ (1990) Architecture of selected wrist flexor and extensor muscles. *J Hand Surg* 15:244–250
13. Lieber RL, Yeh Y, Baskin R (1984) Sarcomere Length Determination Using Laser Diffraction. Effect of Beam and Fiber Diameter. *Biophys J* 1007–016
14. Felder A, Ward SR, Lieber RL (2005) Sarcomere length measurement permits high resolution normalization of muscle fiber length in architectural studies. *J Exp Biol* 208:3275–3279
15. Ward SR, Lieber RL (2005) Density and hydration of fresh and fixed human skeletal muscle. *J Biomech* 38:2317–2320
16. Bodine SC, Roy RR, Eldred E, Edgerton VR (1987) Maximal force as a function of anatomical features of motor units in the cat tibialis anterior. *J Neurophysiol* 57:1730–1745
17. Tirrell TF et al (2012) Human skeletal muscle biochemical diversity. *J Exp Biol* 215:2551–2559
18. Edwards CA, O'Brien WD (1980) Modified assay for determination of hydroxyproline in a tissue hydrolyzate. *Clin Chim Acta* 104:161–167
19. Ward SR, Eng CM, Smallwood LH, Lieber RL (2009) Are current measurements of lower extremity muscle architecture accurate? *Clin Orthop Relat Res* 1074–82
20. Ward SR, Kim CW, Eng CM, Gottschalk LJ 4th, Tomiya A, Garfin SR, Lieber RL (2009) Architectural analysis and intraoperative measurements demonstrate the unique design of the multifidus muscle for lumbar spine stability. *J Bone Joint Surg Am* 91:176–185
21. Brown SH, Ward SR, Cook MS, Lieber RL (2011) Architectural analysis of human abdominal wall muscles: implications for mechanical function. *Spine* 36:355–362
22. Smith MD, Coppieters MW, Hodges PW (2007) Postural response of the pelvic floor and abdominal muscles in women with and without incontinence. *Neurourol Urodyn* 26:377–385
23. Fung YC (1981) *Biomechanics: Mechanical properties of living tissues*. Springer Verlag, New York
24. Cobb WS, Burns JM, Kercher KW, Matthews BD, Norton HJ, Heniford T (2005) Normal intra-abdominal pressure in healthy adults. *J Surg Res* 129:231–235
25. Al-Khan A, Shah M, Altabban M, Kaul S, Dyer KY, Alvarez M, Saber S (2011) Measurement of intra-abdominal pressure in pregnant women at term. *J Redprod Med* 56:53–57
26. Gerten KA, Richeter HE, Wheeler TL, Pair LS, Burgio KL, Redden DT, Varner E, Hibner M (2008) Intra-abdominal pressure changes associated with lifting: implications for postoperative activity restrictions. *Am J Obstet Gynecol* 198:306.e1–306.e5
27. Iqbal A, Haider M, Stadlhuber RJ, Karu A, Corkill S, Filipi CJ (2008) A study of intragastric and intravesicular pressure changes during rest, coughing, weight lifting, retching, and vomiting. *Surg Endosc* 22:2571–2575
28. Ridgeway B, Arias BE, Barber MD (2011) The relationship between anthropometric measurements and the bony pelvis in African American and European American women. *Int Urogynecol J* 22:1019–1024
29. Katz B (1939) The relation between force and speed in muscular contraction. *J Physiol (London)* 96:45–64
30. Morris VC, Murray MP, DeLancey JO, Ashton-Miller JA (2012) A comparison of the effect of age on levator ani and obturator internus muscle cross-sectional areas and volumes in nulliparous women. *Neurourol Urodyn* 31:481–486
31. Lexell J, Taylor CC, Sjoström M (1988) What is the cause of ageing atrophy? Total number, size and proportion of different fiber types studied in whole vastus lateralis muscle from 15–83-year-old men. *J Neurol Sci* 84:275–294